2026 IEEE/SICE International Symposium on System Integration (SII)
January 11-14, 2026. Cancún, México

Position-Based Force Control for In-Hand Manipulation Using a Soft-Rigid Hybrid Two-Finger Hand

Keita Katamine, Hikaru Arita, Kazuto Nakashima, and Kenji Tahara

Abstract— **Soft grippers have attracted attention as a safe and adaptable means of grasping fragile or irregularly shaped objects. However, challenges remain in performing advanced tasks such as in-hand manipulation. This study proposes a soft-rigid hybrid two-finger hand that integrates position-controlled motors and flexible links, based on a design concept that combines the mechanical properties of rigid and flexible components. The proposed hand directly drives the flexible links using position-controlled motors, enabling active control of the interaction between the flexible structure and the environment. Leveraging this feature, a position-based force control strategy is introduced, in which fingertip positions are adjusted to shift the equilibrium of the flexible links, indirectly modulating the contact force through their passive deformation. The effectiveness of the proposed method is validated through simulations of object grasping tasks, demonstrating stable and dexterous in-hand manipulation.**

I. INTRODUCTION

Soft grippers made of soft materials such as polymers are suitable for human collaboration and grasping irregular objects due to their conformability and safety [1], [2], [3]. They are expected to be applied in industries such as agriculture and food handling. The application of soft grippers has recently been extended beyond simple enveloping grasps to more sophisticated tasks such as in-hand manipulation [4], [5]. In-hand manipulation refers to adjusting the position and orientation of a grasped object using fingertip forces while maintaining grasp. If achieved, this would enable both enveloping grasps and in-hand manipulation in a more versatile manner, leading to broader applications of soft grippers. This requires precise force control across multiple contact points and the ability to handle uncertainties such as contact point movement and the friction and stiffness of the object, demanding high-level control performance. However, embedding sensors into flexible components is challenging, making it difficult to accurately measure contact force or deformation. Without precise sensing, it is difficult to obtain the current state necessary for feedback control, forcing soft grippers to rely on open-loop and sensorless control. In such cases, model-based control methods with appropriate state estimation are frequently employed, but soft grippers exhibit strong nonlinearity and uncertainty, making it difficult to accurately model their dynamic behavior [6]. In particular, when linear models are used, large posture changes lead to increased approximation errors, resulting in significant discrepancies between estimated and actual values. Therefore, the combined difficulty of precise sensing and accurate modeling limits the achievement of high-precision manipulation.

Soft-rigid hybrid structures have been introduced to address the limitations of soft grippers. While soft robots are often inspired by flexible biological structures such as elephant trunks or octopus tentacle [7], [8], many real-world organisms utilize tightly integrated rigid and soft tissues [9], [10]. Drawing inspiration from such structures, the soft-rigid hybrid structure has gained attention as a practical robotic design that balances flexibility and controllability, with various implementations recently proposed. Examples include robots combining variable-stiffness continuum modules and rigid joints in series [11], cable-driven robots with internal rigid skeletons covered by soft material [12], and robots embedding rigid structures between soft chambers [13]. However, these robots are primarily designed to enhance stiffness or actuation agility, and to the best of the knowledge, in-hand manipulation while leveraging the passive properties of soft materials have not been achieved, either with soft robots or with soft-rigid hybrid robots.

In this study, we propose a soft-rigid hybrid two-finger hand designed to combine the mechanical properties of rigid and flexible components. The hand integrates high-speed, large-deformation actuation via position-controlled motors with passive contact force responses of flexible links, aiming at achieving both flexibility and controllability. Conventional soft grippers experience geometric and mechanical changes in flexible structures due to environmental interactions, but active control of these states is difficult. In contrast, the proposed hand uses position-controlled motors, less affected by the environment, to actively control flexible links. This enables effective use of interactions between flexible parts and the environment. Exploiting this, we present a position-based force control method. By adjusting fingertip desired positions with position-controlled motors and actively changing flexible link equilibrium points, contact forces are indirectly controlled through passive deformation, enabling in-hand manipulation. Since contact force generation relies on passive deformation, the high viscosity and spatiotemporal resolution of the flexible links naturally suppress vibrations and discontinuities, enabling stable force control.

In what follows, a novel approach to in-hand manipulation is presented from both design and control perspectives: soft-rigid hybrid structures and position-based force control.

All authors are with Kyushu University, Fukuoka 819-0395, JAPAN. K. Katamine, H. Arita, and K. Tahara are with the Department of Mechanical Engineering. K. Nakashima is with the Department of Mechanical Engineering and the Department of Interdisciplinary Informatics. E-mails: katamine@hcr.mech.kyushu-u.ac.jp; [arita, tahara, kazuto]@ieee.org.
This work was partially supported by JSPS KAKENHI Grant Number JP24H00726.

978-1-6654-5784-2/26/$31.00 ©2026 IEEE

Section II describes the design of soft-rigid hybrid two-finger hand. Section III introduces its dynamics and viscoelastic model. Section IV details the position-based force control method for in-hand manipulation. Section V presents simulation results that demonstrate the effectiveness of the proposed approach. Section VI discusses the findings, and Section VII concludes the paper.

II. DESIGN

The proposed soft-rigid hybrid two-finger hand was designed by combining flexible links with position-controlled motors (Fig. 1). Each of the two fingers consists of two flexible links and two rigid joints connected in series. Each joint is driven by a position-controlled motor (XC330-M288-T, Dynamixel) for accurate angle control. Flexible links are 3D printed (AGILISTA3200, KEYENCE) and molded with silicone resin (G1H, KEYENCE), allowing passive deformation upon contact. Focusing on planar motion, the links are designed to be compliant in bending and rigid in depth by adding thickness and slits. Red markers spaced every 20 mm along each flexible link are tracked by an external camera to measure deformation.

III. MODEL

Each finger of the proposed hand consists of rigid joints and flexible links connected in series. A flexible link is generally considered as a continuum with infinite degrees of freedom. To simplify the model, its deformation is approximated using a finite number of pseudo joints. Increasing their number improves accuracy but also raises computational cost and complicates parameter identification. Here, the joints driven by position-controlled motors are defined as active joints, while the joints representing flexible link deformations are defined as passive joints. Thus, each finger is modeled as a lumped multi-joint structure with six joints total: two active and four passive (Fig. 2). Let i denote the finger index; the joint angle vector of the i-th finger is $\boldsymbol{q}_i = [q_{i1}, \ldots, q_{i6}]^\top$, where active joints are $\boldsymbol{q}_{\mathrm{ac},i} = [q_{i1}, q_{i4}]^\top$ and passive joints are $\boldsymbol{q}_{\mathrm{pa},i} = [q_{i2}, q_{i3}, q_{i5}, q_{i6}]^\top$. This section describes the dynamics of grasping with the proposed hand and introduces a viscoelastic model for the passive joints.

A. Dynamics model

Referring to the two-finger robot model by Arimoto [14], the dynamics of object grasping using a two-finger robot with six degrees of freedom are derived. To derive the dynamics, geometric constraint conditions must be considered. First, each fingertip moves on the object surface without slipping and performs a pure rotational motion, which imposes a tangential constraint. Second, the fingertips maintain contact with the object without separation, which imposes a normal constraint. Using these conditions, and based on the kinetic energies of the robot and object, we apply Lagrange's equations of motion. As a result, the equations of motion for each finger can be expressed as follows:

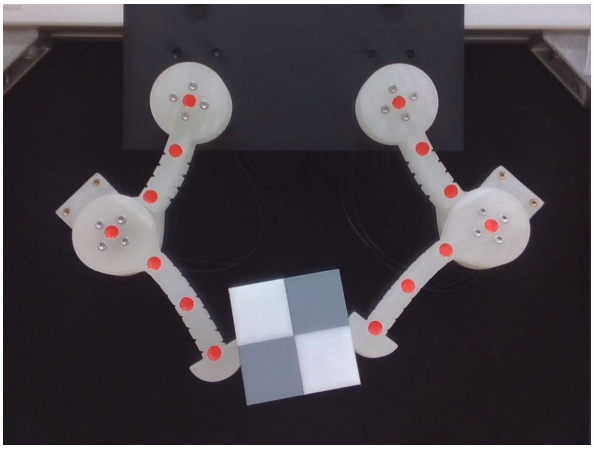

Fig. 1: Prototype of the soft-rigid hybrid two-finger hand.

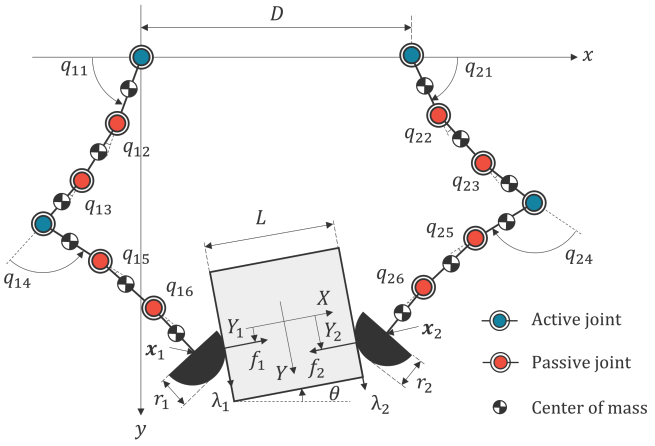

Fig. 2: Lumped parameterized model of a soft-rigid hybrid two-finger hand.

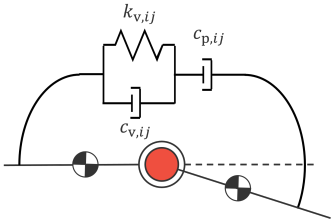

Fig. 3: Viscoelastic three-element model of the passive joint.

$$\boldsymbol{H}_i(\boldsymbol{q}_i)\ddot{\boldsymbol{q}}_i + \boldsymbol{h}_i(\boldsymbol{q}_i, \dot{\boldsymbol{q}}_i) + (-1)^{i-1}\boldsymbol{J}_i^\top \begin{pmatrix} \cos\theta \\ -\sin\theta \end{pmatrix} f_i + \left\{ r_i \begin{pmatrix} 1 \\ 1 \end{pmatrix} - \boldsymbol{J}_i^\top \begin{pmatrix} \sin\theta \\ \cos\theta \end{pmatrix} \right\} \lambda_i = \boldsymbol{\tau}_i \quad (i = 1, 2), \tag{1}$$

where $\boldsymbol{H}_i \in \mathbb{R}^{6\times6}$ is the inertia matrix, $\boldsymbol{h}_i \in \mathbb{R}^6$ is the nonlinear terms, f_i is the contact force in the normal direction between the fingertip and the object, λ_i is the contact force in the tangential direction, θ_i is the orientation angle of the object, and r_i is the fingertip radius. The Jacobian matrix $\boldsymbol{J}_i \in \mathbb{R}^{2\times6}$, which is the derivative of the fingertip position $\boldsymbol{x}_i \in \mathbb{R}^2$ with respect to the joint angles

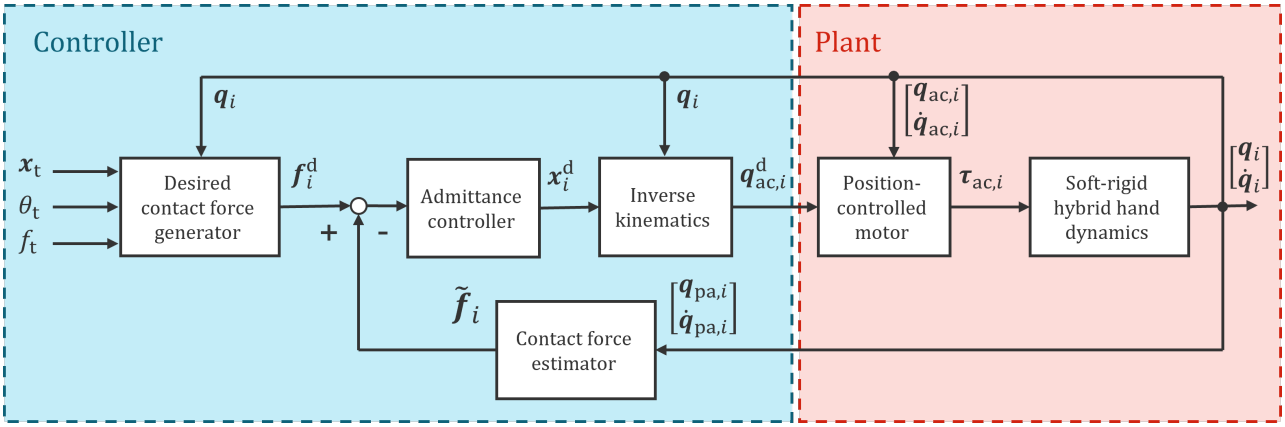

Fig. 4: Block diagram of the object grasping method based on position-based force control.

$\boldsymbol{q}_i$, is defined as follows:

$$\boldsymbol{J}_i = \frac{\partial \boldsymbol{x}_i}{\partial \boldsymbol{q}_i}, \tag{2}$$

where $\boldsymbol{x}_i$ is obtained from forward kinematics. $\boldsymbol{\tau}_i = [\tau_{i1}, \ldots, \tau_{i6}]^\top$ is the joint torque vector, which consists of the active joint torque $\boldsymbol{\tau}_{\mathrm{ac},i} = [\tau_{i1}, \tau_{i4}]^\top$ generated by the position-controlled motor and the passive joint torque $\boldsymbol{\tau}_{\mathrm{pa},i} = -[\tau_{i2}, \tau_{i3}, \tau_{i5}, \tau_{i6}]^\top$ generated by the flexible link. The active joint torque $\boldsymbol{\tau}_{\mathrm{ac},i}$ is expressed as follows:

$$\boldsymbol{\tau}_{\mathrm{ac},i} = \boldsymbol{K}_{\mathrm{ac},i}\left(\boldsymbol{q}_{\mathrm{ac},i}^\mathrm{d} - \boldsymbol{q}_{\mathrm{ac},i}\right) - \boldsymbol{C}_{\mathrm{ac},i}\dot{\boldsymbol{q}}_{\mathrm{ac},i}, \tag{3}$$

where $\boldsymbol{K}_{\mathrm{ac},i} \in \mathbb{R}^{2\times 2}$ is the proportional gain, and $\boldsymbol{C}_{\mathrm{ac},i} \in \mathbb{R}^{2\times 2}$ is the derivative gain. Each gain is set sufficiently large compared to the viscoelasticity of the flexible link. $\boldsymbol{q}_{\mathrm{ac},i}^\mathrm{d} \in \mathbb{R}^2$ denotes the desired angle of the active joints, which serves as the input to the robot. On the other hand, the equation of motion for the object is expressed as follows:

$$M\ddot{x} - (f_1 - f_2)\cos\theta + (\lambda_1 + \lambda_2)\sin\theta = 0, \tag{4}$$

$$M\ddot{y} + (f_1 - f_2)\sin\theta + (\lambda_1 + \lambda_2)\cos\theta = 0, \tag{5}$$

$$I\ddot{\theta} - f_1 Y_1 + f_2 Y_2 + (\lambda_1 - \lambda_2)\frac{L}{2} = 0, \tag{6}$$

where M is the mass of the object, I is the moment of inertia of the object, and L is the width of the object. Y_i represents the distance in the Y-direction, measured in the object coordinate frame, from the center of mass to the fingertip contact point.

B. Viscoelastic three-element model

The deformation of the flexible link exhibits creep behavior continuous deformation under constant external force and transient responses to force changes. To reproduce these characteristics, a three-element viscoelastic model is introduced into the passive joints, consisting of a parallel arrangement of elastic and viscous elements with an additional series viscous element (Fig. 3) [6]. The passive joint torque $\boldsymbol{\tau}_{\mathrm{pa},i}$ is expressed as follows:

$$\boldsymbol{A}_i\dot{\boldsymbol{q}}_{\mathrm{pa},i} + \boldsymbol{B}_i\boldsymbol{q}_{\mathrm{pa},i} = \boldsymbol{C}_i\boldsymbol{\tau}_{\mathrm{pa},i} + \boldsymbol{D}_i\int \boldsymbol{\tau}_{\mathrm{pa},i}\mathrm{d}t, \tag{7}$$

where $k_{\mathrm{v},ij}$, $c_{\mathrm{v},ij}$, and $c_{\mathrm{p},ij}$ represent the parallel elastic element, the parallel viscous element, and the series viscous element, respectively, at the j-th joint of i-th finger. Using these parameters, the coefficient matrices are defined as $\boldsymbol{A}_i = \mathrm{diag}(c_{\mathrm{v},ij}c_{\mathrm{p},ij})$, $\boldsymbol{B}_i = \mathrm{diag}(k_{\mathrm{v},ij}c_{\mathrm{p},ij})$, $\boldsymbol{C}_i = \mathrm{diag}(c_{\mathrm{v},ij} + c_{\mathrm{p},ij})$, $\boldsymbol{D}_i = \mathrm{diag}(k_{\mathrm{v},ij})$. The viscoelastic parameters of each passive joint, $k_{\mathrm{v},ij}$, $c_{\mathrm{v},ij}$, and $c_{\mathrm{p},ij}$, were identified through preliminary experiments. Although the deformation behavior of soft materials is known to exhibit variability across trials [6], these parameters were assumed to be constant to simplify the model. Multiple experiments were conducted, and the median of the estimated values from each trial was adopted as the representative value.

IV. POSITION-BASED FORCE CONTROL FOR IN-HAND MANIPULATION

This study aims to realize in-hand manipulation using a soft-rigid hybrid two-finger hand. To this end, we propose an object grasping method based on position-based force control, in which the desired fingertip position is adjusted through active joint position control, and the contact force is regulated via passive deformation (Fig. 4). The proposed control system consists of three components: generation of the desired contact force $\boldsymbol{f}_i^\mathrm{d} \in \mathbb{R}^2$, calculation of the estimated contact force $\tilde{\boldsymbol{f}}_i \in \mathbb{R}^2$ based on the deformation of passive joints, and calculation of the desired active joint angles $\boldsymbol{q}_{\mathrm{ac},i}^\mathrm{d}$ to make the desired contact force. This section describes the details of these control methods.

A. Desired contact force

The method proposed by Arimoto [14] for stable grasping is employed to generate the desired contact force. The following force control components: the force component $\boldsymbol{f}_{\mathrm{x},i} \in \mathbb{R}^2$ for achieving the target object position $\boldsymbol{x}_\mathrm{t} \in \mathbb{R}^2$, the force component $\boldsymbol{f}_{\mathrm{p},i} \in \mathbb{R}^2$ for achieving the target object orientation θ_t, and the force component $\boldsymbol{f}_{\mathrm{s},i} \in \mathbb{R}^2$ for achieving the target grasping force f_t, are computed as follows:

$$\boldsymbol{f}_{\mathrm{x},i} = -\boldsymbol{K}_\mathrm{x}(\boldsymbol{x}_\mathrm{v} - \boldsymbol{x}_\mathrm{t}), \tag{8}$$

TABLE I: Median of the identified viscoelastic parameters of the passive joint based on the three-element model.

Joint	q_{i2}	q_{i3}	q_{i5}	q_{i6}
k_v ($\mathrm{N \cdot m/rad}$)	0.4307	0.2398	0.2942	0.2630
c_v ($\mathrm{N \cdot m \cdot s/rad}$)	0.7108	0.3651	0.4282	0.4565
c_p ($\mathrm{N \cdot m \cdot s/rad}$)	20.5130	11.5608	15.1282	12.1592

TABLE II: Physical parameters of the robot and the object, where i denotes the finger index and j denotes the link index.

Parameter name	Symbol	Value
Link length	L_{ij}	0.02 (m)
Link mass	M_{ij}	0.004 (kg)
Link mass center	$L_{\mathrm{g},ij}$	0.01 (m)
Link inertia	I_{ij}	1.33×10^{-7} ($\mathrm{kg \cdot m^2}$)
Finger distance	D	0.08 (m)
Fingertip radius	r_i	0.01 (m)
Object width	L	0.04 (m)
Object mass	M	0.02 (kg)
Object inertia	I	5.33×10^{-6} ($\mathrm{kg \cdot m^2}$)
Motor proportional gain	$\boldsymbol{K}_{\mathrm{ac},i}$	$\mathrm{diag}(20, 20)$ ($\mathrm{N \cdot m/rad}$)
Motor derivative gain	$\boldsymbol{C}_{\mathrm{ac},i}$	$\mathrm{diag}(1, 1)$ ($\mathrm{N \cdot m \cdot s/rad}$)

TABLE III: Parameters for desired contact force generation and admittance control.

Parameter name	Symbol	Value
Object position control gain	$\boldsymbol{K}_\mathrm{x}$	$\mathrm{diag}(100, 100)$ (N/m)
Object orientation control gain	K_p	5 (N/rad)
Admittance virtual mass	$\boldsymbol{M}_{\mathrm{adm},i}$	$\mathrm{diag}(0.1, 0.1)$ (kg)
Admittance virtual damping	$\boldsymbol{C}_{\mathrm{adm},i}$	$\mathrm{diag}(20, 20)$ ($\mathrm{N \cdot s/m}$)

$$\boldsymbol{f}_{\mathrm{p},i} = (-1)^i \begin{pmatrix} \sin\theta_\mathrm{v} \\ \cos\theta_\mathrm{v} \end{pmatrix} K_\mathrm{p}(\theta_\mathrm{v} - \theta_\mathrm{t}), \tag{9}$$

$$\boldsymbol{f}_{\mathrm{s},i} = (-1)^i \frac{\boldsymbol{x}_1 - \boldsymbol{x}_2}{\|\boldsymbol{x}_1 - \boldsymbol{x}_2\|} f_t, \tag{10}$$

where $\boldsymbol{K}_\mathrm{x} \in \mathbb{R}^{2\times2}$ and K_p represent proportional gains. The centroid position of the fingertip positions, denoted as $\boldsymbol{x}_\mathrm{v} \in \mathbb{R}^2$, and the orientation angle of the line connecting them, denoted as θ_v, are used as estimates of the object's position and orientation, respectively. By summing the three force control components, the desired contact force $\boldsymbol{f}_i^\mathrm{d}$ for each finger is obtained to achieve the desired object position, orientation, and grasping force, as follows:

$$\boldsymbol{f}_i^\mathrm{d} = \boldsymbol{f}_{\mathrm{x},i} + \boldsymbol{f}_{\mathrm{p},i} + \boldsymbol{f}_{\mathrm{s},i}. \tag{11}$$

B. Contact force estimation

Next, estimated contact force $\tilde{\boldsymbol{f}}_i$ is calculated based on the passive joint angle $\boldsymbol{q}_{\mathrm{pa},i}$ and its velocity $\dot{\boldsymbol{q}}_{\mathrm{pa},i}$ obtained from the camera, as well as a viscoelastic three-element model. Assuming that the viscoelastic parameters of the passive joints are known from preliminary experiments, the estimated passive joint torque $\tilde{\boldsymbol{\tau}}_{\mathrm{pa},i}$ is calculated by rearranging equation (7), as follows:

$$\tilde{\boldsymbol{\tau}}_{\mathrm{pa},i} = \boldsymbol{C}_i^{-1} \left(\boldsymbol{A}_i \dot{\boldsymbol{q}}_{\mathrm{pa},i} + \boldsymbol{B}_i \boldsymbol{q}_{\mathrm{pa},i} - \boldsymbol{D}_i \int \tilde{\boldsymbol{\tau}}_{\mathrm{pa},i} \mathrm{d}t \right). \tag{12}$$

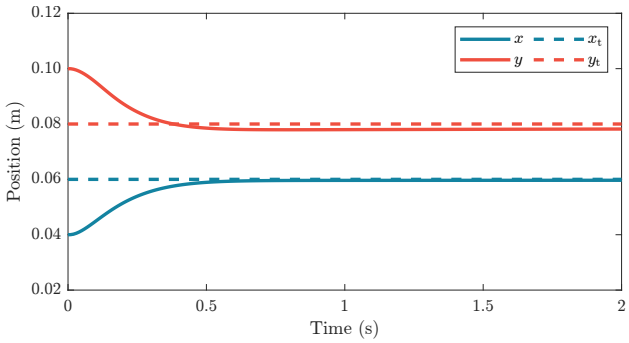

Fig. 5: Time response of the object position.

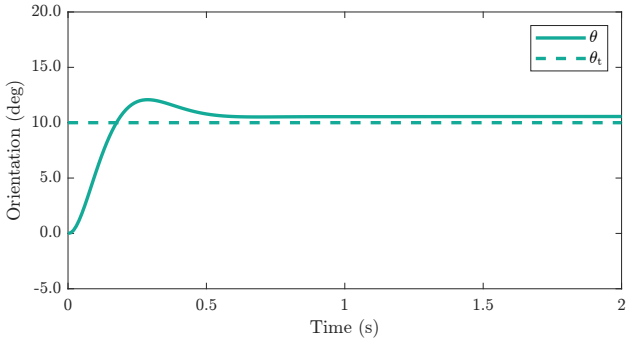

Fig. 6: Time response of the object orientation.

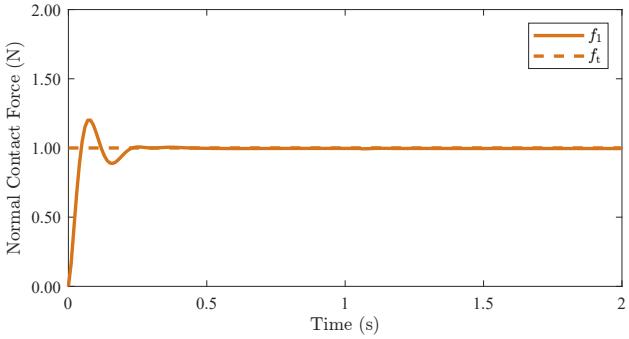

Fig. 7: Time response of the normal cantact force.

Here, the passive joint Jacobian matrix $\boldsymbol{J}_{\mathrm{pa},i} \in \mathbb{R}^{2\times4}$, which is the derivative of $\boldsymbol{x}_i$ with respect to the passive joint angles $\boldsymbol{q}_{\mathrm{pa},i}$, is defined as follows:

$$\boldsymbol{J}_{\mathrm{pa},i} = \frac{\partial \boldsymbol{x}_i}{\partial \boldsymbol{q}_{\mathrm{pa},i}}, \tag{13}$$

where $\boldsymbol{J}_{\mathrm{pa},i}$ is considers only the displacement of the passive joints, neglecting the displacement of the active joints. Using equations (12) and (13), the estimated contact force $\tilde{\boldsymbol{f}}_i$ is calculated based on the pseudoinverse matrix, defined as $\boldsymbol{J}_{\mathrm{pa},i}^+ = \boldsymbol{J}_{\mathrm{pa},i}{}^\top (\boldsymbol{J}_{\mathrm{pa},i} \boldsymbol{J}_{\mathrm{pa},i}^\top)^{-1}$, as follows:

$$\tilde{\boldsymbol{f}}_i = \boldsymbol{J}_{\mathrm{pa},i}^{+\top} \tilde{\boldsymbol{\tau}}_{\mathrm{pa},i}, \tag{14}$$

where equation (14) is not necessarily satisfied $\boldsymbol{J}_{\mathrm{pa},i}^\top \tilde{\boldsymbol{f}}_i = \tilde{\boldsymbol{\tau}}_{\mathrm{pa},i}$. Therefore, $\tilde{\boldsymbol{f}}_i$ is computed to minimize $\|\boldsymbol{J}_{\mathrm{pa},i}^\top \tilde{\boldsymbol{f}}_i - \tilde{\boldsymbol{\tau}}_{\mathrm{pa},i}\|$.

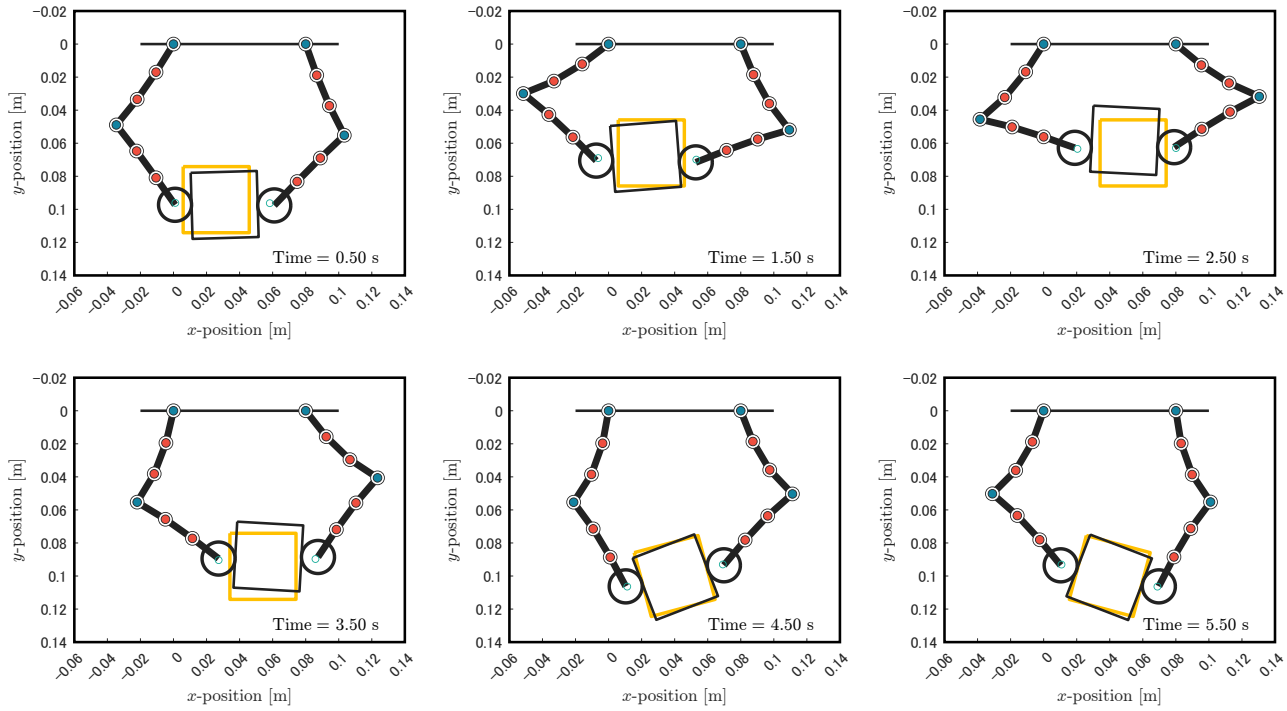

Fig. 8: Simulation snapshots of in-hand manipulation using a lumped-parameter soft-rigid two-finger hand. Blue circles: active joints; red circle: passive joints; black lines: links; black squares: object positions; yellow squares: target positions; green circles: desired fingertip positions.

C. Desired active joint angles via admittance control

Finally, the desired active joint angles are generated so that the fingertip contact force approaches the desired contact force. To this end, the estimated contact force $\tilde{\boldsymbol{f}}_i$ is fed back, and the desired fingertip position $\boldsymbol{x}_i^{\mathrm{d}} \in \mathbb{R}^2$ is computed based on the following admittance control law to approach the desired contact force $\boldsymbol{f}_i^{\mathrm{d}}$, as follows:

$$\boldsymbol{M}_{\mathrm{adm},i}\ddot{\boldsymbol{x}}_i^{\mathrm{d}} + \boldsymbol{C}_{\mathrm{adm},i}\dot{\boldsymbol{x}}_i^{\mathrm{d}} = \boldsymbol{f}_i^{\mathrm{d}} - \tilde{\boldsymbol{f}}_i, \tag{15}$$

where $\boldsymbol{M}_{\mathrm{adm},i} \in \mathbb{R}^{2\times2}$ and $\boldsymbol{C}_{\mathrm{adm},i} \in \mathbb{R}^{2\times2}$ are the inertia and damping matrices that define the virtual dynamics of the desired fingertip position $\boldsymbol{x}_i^{\mathrm{d}}$ in the admittance control, and they are treated as hyperparameters. To realize the computed desired fingertip position $\boldsymbol{x}_i^{\mathrm{d}}$, the active joint Jacobian matrix $\boldsymbol{J}_{\mathrm{ac},i} \in \mathbb{R}^{2\times2}$, which is the derivative of $\boldsymbol{x}_i$ with respect to the active joint angles $\boldsymbol{q}_{\mathrm{ac},i}$, is defined as follows:

$$\boldsymbol{J}_{\mathrm{ac},i} = \frac{\partial \boldsymbol{x}_i}{\partial \boldsymbol{q}_{\mathrm{ac},i}}, \tag{16}$$

where $\boldsymbol{J}_{\mathrm{ac},i}$ considers only the displacement of the active joints, neglecting the displacement of the passive joints. Using equations (15) and (16), the desired active joint angles $\boldsymbol{q}_{\mathrm{ac},i}^{\mathrm{d}}$ are obtained by iteratively solving the inverse kinematics until the following equation converges:

$$\boldsymbol{q}_{\mathrm{ac},i}^{\mathrm{d}} \leftarrow \boldsymbol{q}_{\mathrm{ac},i}^{\mathrm{d}} + \boldsymbol{J}_{\mathrm{ac},i}^{-1}\left\{\boldsymbol{x}_i^{\mathrm{d}} - \boldsymbol{x}_i(\boldsymbol{q}_{\mathrm{ac},i}^{\mathrm{d}})\right\}. \tag{17}$$

The computed desired active joint angles $\boldsymbol{q}_{\mathrm{ac},i}^{\mathrm{d}}$ are applied to high-gain position-controlled motors.

V. SIMULATION

A grasping simulation using position-based force control was conducted with the soft-rigid hybrid two-finger hand. First, the transient response when grasping the object with desired position, orientation, and force was evaluated, confirming convergence to the target values. Then, the object was commanded to follow a given trajectory, demonstrating smooth tracking. In all simulations, the object's initial state was set to $\boldsymbol{x} = [0.04, 0.1]^\top$ m and $\theta = 0$ deg, and the fingertips were initially placed at contact points on the object surface at $Y_i = 0$ m. The initial active joint angles $\boldsymbol{q}_{\mathrm{ac},i}$ were computed via inverse kinematics, while the passive joint angles were initialized as $\boldsymbol{q}_{\mathrm{pa},i} = 0$ deg. The initial desired fingertip positions $\boldsymbol{x}_i^{\mathrm{d}}$ were set equal to the initial fingertip position. The viscoelastic parameters (Table I) and physical parameters (Table II) are identical to those of the two-finger prototype (Fig. 1). The control parameters (Table III) are determined through trial and error to suppress overshoot and achieve fast, smooth convergence.

A. Transient response during grasping

The transient response during grasping with the desired position, orientation, and grasping force is evaluated. The target position is set to $\boldsymbol{x}_{\mathrm{t}} = [0.06, 0.08]^{\mathsf{T}}$ m, the target orientation to $\theta_{\mathrm{t}} = 10$ deg, and the target grasping force to $\boldsymbol{f}_{\mathrm{t}} = 1$ N. Although the variation of the contact point caused by rolling contact introduces slight deviations in the estimated position and orientation, resulting in small steady-state errors in the actual values, both the position and

orientation of the object are confirmed to stably converge to the vicinity of the target within approximately 0.5 s (Fig. 5, 6). In addition, although a transient overshoot occurs at the moment of contact, the grasping force also converges to the target within approximately 0.2 s (Fig. 7). These results demonstrate that the proposed position-based force control enables stable control of position, orientation, and grasping force simultaneously.

B. Trajectory tracking

To evaluate the tracking performance of the proposed control scheme for arbitrary trajectories, a target grasping force of $f_{\mathrm{t}} = 1$ N was applied, and the object was controlled to follow predefined time-varying trajectories of target position $\boldsymbol{x}_{\mathrm{t}}(t)$ and orientation $\theta_{\mathrm{t}}(t)$, as follows:

$$\boldsymbol{x}_{\mathrm{t}}(t) = \begin{cases} \begin{bmatrix} 0.04 - 0.02\sin\left(\dfrac{\pi}{2}t\right) \\ 0.08 + 0.02\cos\left(\dfrac{\pi}{2}t\right) \end{bmatrix} & (0 \le t < 4) \\ \begin{bmatrix} 0.04 \\ 0.10 \end{bmatrix} & (t \ge 4) \end{cases}, \quad (18)$$

$$\theta_{\mathrm{t}}(t) = \begin{cases} 0 & (0 \le t < 4) \\ \dfrac{\pi}{12}\sin\left(\pi(t-4)\right) & (t \ge 4) \end{cases}. \quad (19)$$

The fingertip positions were appropriately adjusted by the position-controlled motors, and the object smoothly followed the target trajectory through passive deformation of the flexible links, exhibiting continuous changes in both position and orientation (Fig. 8).

VI. DISCUSSION

A. Significance of the soft-rigid hybrid structure

Soft robot hands with pneumatic or tendon-driven actuation actively drive flexible components but inherently suffer from response delays and high damping, limiting high-speed manipulation. In contrast, the proposed hand uses high-gain position-controlled motors on rigid joints to rapidly and accurately adjust the flexible structure's equilibrium, achieving high responsiveness. Contact force is generated by passive deformation of flexible links, whose high viscosity naturally suppresses force discontinuities and vibrations, ensuring stable force control. These features balance flexibility and controllability.

B. Limitations and extensions

This study evaluated the soft-rigid hybrid two-finger hand using a lumped-parameter model with constant viscoelastic parameters. However, actual soft materials exhibit trial-to-trial variations [6], and their deformations involve infinite degrees of freedom, leading to modeling discrepancies compared to real-world robots. Future work will involve probabilistic modeling of viscoelastic parameter variability and the introduction of contact force estimation based on state estimation that accounts for parameter uncertainty [15], aiming to improve accuracy and robustness in physical systems. Furthermore, although this study focused solely on bending deformation using a two-dimensional model, extending it to include axial and torsional deformations would enable application to three-dimensional hands, facilitating a wider range of manipulation tasks.

VII. CONCLUSION

In this study, a soft-rigid hybrid two-finger hand with position-controlled motors and flexible links was used, and a position-based force control method for in-hand manipulation was proposed. The proposed method enables in-hand manipulation using a soft-rigid hybrid two-finger hand, allowing simultaneous control of the object's position, orientation, and grasping force, as well as tracking of arbitrary trajectories. These capabilities were demonstrated through simulations based on a lumped-parameter approximation model. Future work includes introducing probabilistic models to handle deformation uncertainties and validating the approach with a physical prototype.

REFERENCES

[1] C. Lee, M. Kim, Y. J. Kim, N. Hong, S. Ryu, H. J. Kim, and S. Kim: "Soft Robot Review," International Journal of Control, Automation and Systems, vol. 15, no. 1, pp.3–15, 2017.

[2] Y. Wang, G. Wang, W. Ge, J. Duan, Z. Chen, and L. Wen: "Perceived Safety Assessment of Interactive Motions in Human–Soft Robot Interaction," Biomimetics, vol. 9, no. 1, 58, 2024.

[3] J. Shintake, V. Cacucciolo, D. Floreano, and H. Shea: "Soft robotic grippers," Advanced materials, vol. 30, no. 29, 1707035, 2018.

[4] A. Pagoli, F. Chapelle, J. A. Corrales, Y. Mezouar, and Y. Lapusta: "A Soft Robotic Gripper With an Active Palm and Reconfigurable Fingers for Fully Dexterous In-Hand Manipulation," IEEE Robotics and Automation Letters, vol. 6, no.4, pp. 7706–7713, 2021.

[5] S. Abondance, C. B. Teeple, and R. J. Wood: "A Dexterous Soft Robotic Hand for Delicate In-Hand Manipulation," IEEE Robotics and Automation Letters, vol. 5, no.4, pp. 5502–5509, 2020.

[6] S. Honji, H. Arita, and K. Tahara: "Stochastic approach for modeling soft fingers with creep behavior," Advanced Robotics, vol. 37, no. 22, pp. 1471–1484, 2023.

[7] . Leanza, J. Lu-Yang, B. Kaczmarski, S. Wu, E. Kuhl, and R. R. Zhao: "Elephant Trunk Inspired Multimodal Deformations and Movements of Soft Robotic Arms," Advanced Functional Materials, vol. 34, no. 29, 2400396, 2024.

[8] Z. Xie, F. Yuan, J. Liu, L. Tian, B. Chen, Z. Fu, S. Mao, T. Jin, Y. Wang, X. He, G. Wang, Y. Mo, X. Ding, Y. Zhang, C. Laschi, and L. Wen: "Octopus-inspired sensorized soft arm for environmental interaction," Science Robotics, vol. 8, no. 84, 7852, 2023.

[9] R. W. Blob, N. R. Espinoza, M. T. Butcher, A. H. Lee, A. R. D'Amico, F. Baig, and K. M. Sheffield: "Diversity of Limb-Bone Safety Factors for Locomotion in Terrestrial Vertebrates: Evolution and Mixed Chains," Integrative and Comparative Biology vol. 54, no. 6, pp. 1058—1071, 2014.

[10] T. J. Roberts and E. Azizi: "Flexible mechanisms: The diverse roles of biological springs in vertebrate movement," Journal of Experimental Biology, vol. 214, no. 3, pp. 353—361, 2011.

[11] Z. J. Patterson, E. Sologuren, C. Della Santina, and D. Rus: "Design and Control of Modular Soft-Rigid Hybrid Manipulators with Self-Contact," arXiv preprint arXiv:2408.09275v1, 2023.

[12] J. M. Bern, F. Zargarbashi, A. Zhang, J. Hughes, and D. Rus: "Simulation and Fabrication of Soft Robots with Embedded Skeletons," IEEE International Conference on Robotics and Automation, pp. 5205–5211, 2022.

[13] W. Park, S. Seo, and J. Bae: "A Hybrid Gripper With Soft Material and Rigid Structures," IEEE Robotics and Automation Letters, vol.4, no.1, pp. 65–72, 2019.

[14] S. Arimoto: "Control Theory of Multi-fingered Hands: A Modelling and Analytical–Mechanics Approach for Dexterity and Intelligence," Springer London, 2008.

[15] S. Honji, H. Arita, and K. Tahara: "State Estimation of a Soft Robotic Finger with Dynamic Effect of Parameter Uncertainty," IEEE International Conference on Soft Robotics, pp. 444–451, 2024.